Journal of Atmospheric and Solar-Terrestrial Physics 179 (2018) 40–54

Contents lists available at ScienceDirect

Journal of Atmospheric and Solar-Terrestrial Physics

journal homepage: www.elsevier.com/locate/jastp

Decadal variability in the Northern Hemisphere winter circulation: Effects of different solar and terrestrial drivers

Ville Maliniemi*, Timo Asikainen, Kalevi Mursula

ReSoLVE Centre of Excellence, Space Climate Research Unit, University of Oulu, Finland

ARTICLE INFO

Keywords:
ENSO
Volcanic activity
Solar activity
QBO
Surface circulation
Northern hemisphere winter

ABSTRACT

Northern Hemisphere winter circulation is affected by both solar and terrestrial forcings. El-Niño events and volcanic eruptions have been shown to produce a negative and a positive North Atlantic Oscillation (NAO) signature, respectively. Recent studies show a positive NAO signature related to both geomagnetic activity (proxy for solar wind driven particle precipitation) and sunspot activity (proxy for solar irradiance). Here the relative role of these four different drivers on the Northern Hemisphere wintertime circulation is studied using a statistical analysis of observational and reanalysis data during 1868–2014. The phase of the Quasi-Biennial Oscillation (QBO) is used to study driver signals in different stratospheric conditions. Moreover, the effects are separated for early/mid- and late winter. Our findings suggest a stratospheric mediation of the ENSO signal to the Atlantic side, which is delayed and modulated by the QBO unlike the signal in the Pacific side. The positive NAO by volcanic activity is preferentially obtained in the westerly QBO. We also find a substantial QBO modulation for geomagnetic activity and late winter sunspot activity, which favours a stratospheric pathway and the top-down mechanisms. However, signal in the North Pacific produced by early/mid-winter sunspot activity remain rather similar in different QBO phases and supports a direct forcing from the troposphere by the bottom-up sunspot mechanism.

1. Introduction

Winter conditions at high-latitudes of the Northern Hemisphere are known to be affected by several climatic variables. ENSO (El-Niño Southern Oscillation) has been shown to affect European winter conditions at least since the early 1700s (Brönnimann et al., 2007b). Huang et al. (1998) have shown that there exists a significant coherence between ENSO and the North Atlantic Oscillation (NAO) during the 20th century. Positive ENSO (El-Niño) events have been shown to cause a negative NAO response (Pozo-Vázquez et al., 2001). On the other hand, this response has been found to be dependent on the strength of the ENSO event (Toniazzo and Scaife, 2006). Moderate El-Niño events have been shown to produce a negative NAO by intensifying the propagation of Pacific extra-tropical stationary planetary waves to the stratosphere and weakening the polar vortex (Bell et al., 2009). During the strongest El-Niño events the stratospheric pathway is saturated and forcing through the tropospheric tropical Atlantic produces a feature that resembles a positive NAO in Western Europe (Bell et al., 2009). Recently, Herceg-Buli et al. (2017) have shown that the ENSO signal in the North Atlantic can experience a lag so that in springtime it consists of a direct forcing from the stratosphere and a delayed forcing generated by the atmosphere-ocean interaction. Ineson and Scaife (2009) have also shown that the downward progression of an ENSO signal from the stratosphere reaches the surface level of the Atlantic in late winter (Feb/Mar) with a few months delay relative to the stratospheric signal.

Other significant contributors to the winter conditions in the Northern Hemisphere are volcanic eruptions (Fischer et al., 2007). Major volcanic eruptions are typically followed by global cooling because of the enhanced scattering of incoming solar radiation (Robock, 2000). On the other hand, warm conditions in European winter dominate after volcanic eruptions and a positive NAO response is observed over the Northern Hemisphere (Shindell et al., 2004). This is due to enhanced heating of the lower equatorial stratosphere in the volcanic aerosol layer, which leads to increased meridional temperature gradient and acceleration of the polar vortex (Otterå et al., 2010).

Two different types of solar activity-related drivers are connected to NAO surface signals, the solar irradiance related variations (Gray et al., 2010) and the solar wind-related variations (Seppälä et al., 2014). Solar irradiance (TSI and solar EUV/UV) variations roughly follow the sunspot cycle (Lockwood and Fröhlich, 2007), although recent observations have proposed that some other parts of the solar spectrum can vary differently (Ermolli et al., 2013). Enhanced solar UV irradiance

* Corresponding author.
E-mail address: ville.maliniemi@oulu.fi (V. Maliniemi).

https://doi.org/10.1016/j.jastp.2018.06.012
Received 26 February 2018; Received in revised form 21 June 2018; Accepted 22 June 2018
Available online 27 June 2018

during sunspot maximum years increases ozone production in the equatorial stratosphere (Haigh, 2007), leading to enhanced equatorial heating and larger meridional temperature gradient (Frame and Gray, 2010; Mitchell et al., 2015). This intensifies stratospheric westerly winds in the winter at mid to high latitudes (Mitchell et al., 2015) due to the thermal wind balance (Holton, 2004). Changes in the polar vortex strength are known to affect the surface circulation (Baldwin and Dunkerton, 2001; Kidston et al., 2015). In the context of solar forcing, this mechanism is often called the top-down mechanism (Kodera and Kuroda, 2002). Thiéblemont et al. (2015) suggested that this top-down mechanism synchronizes an intrisic decadal mode of the NAO, leading to a positive NAO signal in the years following solar maximum.

In addition, another forcing related to solar irradiance called the bottom-up mechanism is operating in the Pacific region (Cubasch et al., 1997; Meehl et al., 2008). It enhances the trade winds and produces a stronger ITCZ (intertropical convergence zone) due to increased total solar irradiance (TSI) energy input on the surface at cloud-free areas during sunspot maximum. This is seen in the surface temperature as a La-Niña type feature and as a positive sea-level pressure (SLP) anomaly in the Aleutian region (van Loon et al., 2007). Note however that this mechanism might be sensitive to the chosen time period (Roy and Haigh, 2012).

Another pathway whereby solar forcing can act terrestrial climate is by the high speed solar wind streams from coronal holes, which typically maximizes a few years after sunspot maximum (Mursula et al., 2015). The flux of magnetospheric energetic particles (Asikainen and Ruopsa, 2016) and the level of geomagnetic activity closely follow the solar wind speed. Enhanced energetic particle precipitation into the upper polar atmosphere during polar night produces reactive nitrogen (Funke et al., 2014) and hydrogen oxides (Andersson et al., 2014), which can destroy ozone in the mesosphere and the upper stratosphere in catalytic reactions (Rozanov et al., 2012; Andersson et al., 2014; Fytterer et al., 2015a; b; Arsenovic et al., 2016). This leads to thermal and dynamical changes in the stratosphere, accelerating the polar vortex (Baumgaertner et al., 2011; Seppälä et al., 2013) and enhancing the positive NAO (Maliniemi et al., 2016).

Long-term surface climate records have shown that the positive NAO conditions are systematically observed during the declining phase of the sunspot cycle when geomagnetic activity typically maximizes (Maliniemi et al., 2014). In addition, the long-term relation between geomagnetic activity and the NAO is better observed in late winter (Maliniemi et al., 2016). The descent of NO_x from the thermosphere/mesosphere can take months to reach the stratosphere (Funke et al., 2014). Seppälä et al. (2013) have noted that due to this delay, the late winter is affected by precipitation from the early winter, and geomagnetic forcing after January is less likely to result in a significant effect. Lu et al. (2008) have shown that zonal wind and temperature anomalies related to solar wind variability are stronger later in winter with a lag of a few months.

The quasi-biennial oscillation (QBO) operates in the equatorial stratosphere, affecting also the extra-tropical stratosphere and the strength of the polar vortex. The polar vortex is stronger (weaker) during the westerly (easterly) QBO phase (Holton and Tan, 1980, 1982; Anstey and Shepherd, 2014). This Holton-Tan effect is explained by the poleward movement of zero wind line during the easterly QBO, which guides planetary waves more to the high latitudes (Baldwin et al., 2001). Flury et al. (2013) have shown that the speed of the Brewer-Dobson circulation depends on the QBO phase so that the vertical speed in the tropical stratosphere is stronger during the easterly QBO measured at 30 hPa. Polar vortex strength and the Brewer-Dobson circulation are usually strongly anticorrelated, both depending strongly on the wave forcing in the stratosphere (Salby and Callaghan, 2003). The QBO has also been shown to control the sunspot (Labitzke and van Loon, 1988; Roy and Haigh, 2011) and the solar wind related (Maliniemi et al., 2016) signals in the troposphere, as well as the ENSO forcing of the Northern Hemisphere (Calvo et al., 2009; Hansen et al., 2016).

In this paper we study the statistical relationship of winter surface circulation (SLP and zonal wind) to ENSO, volcanic activity, geomagnetic activity and sunspot activity from the late 19th century to the modern times using a multilinear regression. Earlier studies have indicated that a notable variability in direct and lagged signal related to ENSO (Herceg-Buli et al., 2017), geomagnetic activity (Maliniemi et al., 2016) and sunspot activity (Gray et al., 2016) can exist within a winter. For this reason we study early/mid-winter (Dec–Jan) and late winter (Feb–Mar) separately allowing the possible lagged signals to emerge. In addition, we also study the effect of the above mentioned four forcings in the two QBO phases separately. This allows us to make tentative conclusions on how the different forcings are mediated and whether the stratosphere plays a major role. The paper is organized as follows. In Section 2 we present the data and the methods. In Section 3 we discuss the SLP results in early and late winter, and in Section 4 the effect of the QBO phase. Section 5 presents the results for the zonal wind. Conclusions are given in Section 6.

2. Data sets and statistical methods

We use the monthly SLP observations by the Hadley center (Allan and Ansell, 2006), available since 1850, and the 20th century reanalysis surface zonal wind (ZW) data (Compo et al., 2011), available since 1851, representing surface circulation during winter. Both of these data sets are gridded in latitude-longitude bins (5° × 5° for SLP and 2° × 2° for ZW) over the whole globe. The monthly Nino3.4 index of sea surface temperature (averaged over 5N-5S and 170W-120W) from NOAA, available since 1856, is used to represent ENSO. Volcanic activity is represented by the updated stratospheric optical depth data by NASA (Sato et al., 1993) averaged over the Northern Hemisphere. (This data is available since 1850 and we have extended this series from the end of 2012 to the end of 2014 with zero values). QBO at 30 hPa height is obtained from the long-term reconstruction by Brönnimann et al. (2007a), which extends to year 1900. This reconstruction is based on relatively sparse observations of ozone and balloon measurements before the 1950s and thus includes considerable uncertainty in the early 20th century. Yet, Brönnimann et al. (2007a) state that it captures reasonably well the maximum phases of the QBO already since 1910.

The sunspot number (SSN) is used as a proxy for total and UV solar irradiances. Sunspot data for monthly resolution extends to year 1749. Earlier studies have shown that solar TSI and UV closely follow sunspot activity (see e.g. Lockwood and Fröhlich, 2007) at monthly and longer timescales. Monthly averaged aa index of geomagnetic activity is used as a proxy for solar wind and particle precipitation related activity. This data is available since 1868 and is defined by the measurements from two stations, located in South England (Greenwich 1868–1925, Abinger 1926–1956 and Hartland 1957-) and Southeast Australia (Melbourne 1868–1919, Toolangi 1920–1979 and Canberra 1980-).

The solar dynamo defines the magnetic activity of the Sun and consists of two components, the toroidal and the poloidal phase (Ruzmaikin and Feynman, 2001). Sunspot activity follows the toroidal phase, whereas solar wind speed is related to the poloidal phase (Ruzmaikin and Feynman, 2001). Geomagnetic activity has contribution from both the toroidal and the poloidal phase, and we use the method introduced by Feynman (1982) to separate these contributions. Thus, the poloidal aa index (aa*) for Dec/Jan is obtained as $aa^* = aa - 0.0515 \times SSN - 6.3$, which removes the toroidal component from the aa index. Thereafter, the poloidal component aa* has only marginal correlation (0.09) with SSN, whose correlation with the Dec/Jan averages of the original aa index is 0.48 (p-value < 0.01) during 1868–2014. The correlation between the original aa index and the aa* index for the same time period is still very high (0.91, p-value < 0.01), which shows that the poloidal component dominates geomagnetic activity.

We use a multilinear regression with four explaining variables: the Nino3.4 index, the stratospheric optical depth, the aa* index and the

SSN. In each 5° × 5° (2° × 2°) SLP (ZW) bin of the whole Northern Hemisphere regression is calculated over the whole time period of 1868–2014 (since the start of the aa index). Regression is performed using the Cochrane-Orcutt method (Cochrane and Orcutt, 1949). In this method the residual term is modeled as an autoregressive AR(1) process instead of white noise as in regular regression. Thus the regression model is

$$y_t = \alpha + \sum_{i=1}^{k} \beta_i X_{i,t} + \varepsilon_t, \quad (1)$$

where k is the number of explaining variables and the residual term is $\varepsilon_t = \rho\varepsilon_{t-1} + e_t$ with ρ being the lag-1 autocorrelation of the residual and e_t being normally distributed white noise. The above regression model can be written as

$$y_t - \rho y_{t-1} = \alpha(1-\rho) + \sum_{i=1}^{k} \beta_i (X_{i,t} - \rho X_{I,t-1}) + e_t. \quad (2)$$

The regression parameters and ρ can be solved iteratively by first performing normal regression for 1 and estimating ρ from the residual time series ε_t. Then regression is performed for 2 using the value of ρ obtained in the previous step. After that a new estimate for ρ can be obtained from the new residuals. The procedure of estimating regression parameters from 2 and then ρ can be iterated until ρ converges. Because the residual term of Eq. (2) is uncorrelated white noise the variances and statistical significance of the regression parameters of Eq. (2) can then be estimated with a standard two-tailed Student's t-test (note that for Eq. (1) Student's t-test would be inappropriate due to the AR(1) noise). This method of regression takes into account the autocorrelation of variables. Furthermore, it is particularly suitable for problems, where the model residual may also contain a physical signal from some other factors, which can possess significant autocorrelation but are explicitly omitted from the model. Their effects can implicitly be modeled by the autoregressive residual term. Therefore, signals from other omitted variables cannot leak to the used explaining variables.

Two different two-month averages are used for the winter period: December/January (the early/mid-winter) and February/March (the late winter). All explaining variables for both cases are calculated as December/January averages, so there is a two-month lag in the late winter signal relative to the explaining variables. This procedure allows us to study a possible direct and a delayed signal relative to each explaining variable. Evidence already cited in the introduction supports this choice at least for ENSO, aa* and SSN.

Before calculating the regressions the long-term trend of ENSO, volcanic activity, aa* index, SSN, SLP and ZW data are removed. Smoothly varying (two-month average) trends are calculated with a LOWESS-method (LOcally WEighted Scatterplot Smoothing, Cleveland and Devlin (1988)) with a 31-year window, which is then subtracted from the considered two-month average time series. (More information about the trend removal procedure can be obtained in Maliniemi et al., 2014). Removing the long-term trend guarantees that the results represent mainly the inter-annual (decadal) variability rather than being dominated by the long-term change in the data. Note also, that because of this, the ocean related multidecadal climate drivers, the Pacific Decadal Oscillation (PDO) and the Atlantic Multidecadal Oscillation (AMO), have been left out of this study. The QBO is not detrended since it is not an explaining variable but rather we want to study the effect of explaining variables in different QBO phases, and the easterly (negative) QBO values have typically a larger amplitude than the westerly (positive) QBO (see A1). After the trend removal, the explaining variables are standardized before calculation. Thus, the results in Figs. A3-A10 show the range of SLP (ZW) variation in hPa (m/s) corresponding to one standard deviation increase of each explaining variable.

Fig. A1 shows the Dec/Jan time series of each explaining variable since 1868 as well as the QBO since 1900. One can see that volcanic activity is dominated by two clusters of large eruptions in the turn of the 19th to 20th century and in the late 20th century. The aa* peaks typically a few years after sunspot maximum in the declining phase of the sunspot cycle. Fig. A2 shows the Dec/Jan (Feb/Mar) climatologies of SLP and ZW during 1868–2014 (1869–2014). One can see that the SLP climatology consists of two low pressure centers around Iceland and Aleutian, which are surrounded by high pressure areas. The Asian continent is dominated by the Siberian high.

Zonal wind climatology consists of westerly jets roughly between the polar and the Ferrell cells in the oceanic regions and easterly jets corresponding to trade winds at low/mid-latitudes. Thus, ZW climatology shows westerlies (easterlies) in the oceanic areas where pressure gradient is negative (positive) polewards. Note that there are wave-like structures in the ZW climatology. These are a consequence of a spectral transformation in the corresponding 20th century reanalysis model (G. P. Compo, personal communication, 2017). Thus, one must note this uncertainty inherent in the current ZW data when analyzing the results. (Future version of the data will be purified from this effect; G. P. Compo, personal communication, 2017). We use this data because it provides considerably longer time series compared to the other modern reanalysis data sets, which allows us to directly compare it to our SLP results with the same temporal coverage.

3. Long-term SLP signal in early/mid- and late winter

Fig. A3 shows the different regression coefficients for SLP during early/mid-winter (Dec/Jan) for the time period of 1868–2014. One can see that each of he explaining variables has a significant signature in some parts of the Northern Hemisphere. The largest effect comes from ENSO variability which shows large negative anomalies over the Northern Pacific and the Western Atlantic and a smaller positive anomaly over the Arctics. There is also a large positive anomaly at low latitudes, especially in the West Pacific. Overall, the ENSO effect has features which project negatively to the hemispheric northern annular mode (NAM) pattern, in agreement with earlier studies (see e.g., Roy and Haigh, 2011; Gray et al., 2013). The volcanic activity signal is seen as a significant negative SLP anomaly over the Arctics, which has been also observed earlier in similar studies (Roy and Haigh, 2011; Gray et al., 2013).

The signal due to aa* index is seen as a significant negative signal around Scandinavia and the Barents Sea and a positive signal at the mid-Atlantic (Azores). This signal resembles the positive NAO pattern but with a slight shift of NAO pressure centers to the northeast. In fact, NAO pressure centers are known to have long-term shifts (Wang et al., 2012). There is also a significant negative signal to aa* at North Pacific around Aleutian. SSN produces a significant positive signal in the North Pacific and a weak negative signal around South/Mid Eurasia. These patterns of SSN and aa* are very similar to the patterns observed in an earlier regression study which used geomagnetic and sunspot activity as separate drivers (Roy et al., 2016). Our results verify that these signals remain significant when both drivers are simultaneously included in the MLR model, and that the aa* index signature on surface climate is observed even after removing the sunspot related variability from the aa index. The total explained variance of SLP by these four variables in the regions of interest vary between 20 and 30% in the North Atlantic and around 30–40% in the North Pacific, with higher values in the low latitudes related to ENSO.

Fig. A4 shows the regression coefficients of ENSO, volcanic activity, aa* and SSN in late winter (Feb/Mar) SLP during 1869–2014. One can see that in late winter the ENSO signal in the Pacific sector is very similar to early/mid-winter. However, in the Atlantic sector and over the Arctic the signal is much stronger and more extended than in early/mid-winter. This implies that there is a lag of a few months for the ENSO signal to reach the Atlantic sector from the Pacific. This supports the idea that the ENSO response in the Atlantic is mediated through planetary wave forcing of the stratosphere/upper troposphere later in winter (Huang et al., 1998; Ineson and Scaife, 2009), whereas strong

signal in the North Pacific forms earlier and is of a direct tropospheric origin. Interestingly, while the global pattern of the volcanic activity signal in late winter remains the same, there is hardly any region of significant signal. The strong negative signal in the Arctic in early winter is reduced in size and remains below statistical significance.

The SLP signature to aa* in late winter remains roughly the same in the Atlantic as in early winter, although it is shifted further to the northeast. Signature in the North Pacific disappears in late winter. Seppälä et al. (2013) have shown that geomagnetic activity effect to the polar vortex was significantly observed between December and March, which is in line with our findings that show a significant pressure dipole structure in both early/mid- and late winter (although shifted northwards) related to aa*. The late winter signal in SSN is very different from the early/mid-winter signal so that a strong positive signal in the North Pacific is replaced by a weaker negative signal. There is also a strong negative signal over the Arctic and a weak positive signal over South Europe, which project positively to the NAO pattern. Note, however, that there is only a weak positive signal to sunspot activity in the mid-to low latitude Atlantic sector in late winter.

The difference between the early/mid-winter and the late winter SSN signals is notable and suggests that the mechanisms behind these signatures are different. Indeed, the positive pressure anomaly in the North Pacific in Fig. A3 resembles very much results obtained earlier for the bottom-up mechanism operating in the Pacific (van Loon et al., 2007; Meehl et al., 2008). Late winter signal instead supports the solar UV effect to circulation in the Atlantic region, the so called top-down effect (Ineson et al., 2011). This is also in line with the ENSO notion above, implying that forcing via the stratosphere takes a bit longer to progress than the direct forcing from the lower troposphere.

4. Long-term SLP signal in different QBO phases

In order to study the QBO dependence, we divide the data into years of easterly (< 0) and westerly (> 0) QBO phase. Dec/Jan mean QBO at 30 hPa is used for both early/mid- and late winter cases. Fig. A5 shows the signature to the four explaining variables in the two QBO phases in early/mid-winter during 1900–2014 (67 winters in the easterly QBO phase and 48 winters in the westerly QBO phase). One can see that the ENSO signal is quite similar in the Pacific in both QBO phases. However, in the Atlantic region ENSO in easterly QBO projects to a wide negative NAO pattern, whereas in westerly QBO ENSO projects positively to the NAO pattern. Ineson and Scaife (2009) have shown that the ENSO response in the Atlantic sector depends on the state of the stratosphere, causing a negative NAO pattern only during a weaker polar vortex. They propose that when sudden stratospheric warmings (SSW) modulate the polar vortex, planetary waves generated by the North Pacific ENSO signal can propagate better to the stratosphere causing further modulation to the polar vortex. Results in Fig. A5 agree with this, especially by noting that the polar vortex is weaker during the easterly QBO in early winter (Holton and Tan, 1980; Maliniemi et al., 2016).

The pattern related to volcanic activity is spatially roughly the same in both QBO phases but slightly stronger, and more closely resembling the positive NAO pattern in the westerly QBO. Volcanic eruptions tend to heat the lower equatorial stratosphere due to the enhanced absorption of infrared radiation by volcanic aerosols (Robock, 2000; Otterå et al., 2010). This increases the pole-to-equator temperature gradient and thus enhances the polar vortex (Otterå et al., 2010). We propose that the stronger surface signal in the westerly QBO could be due to the different effect of the Brewer-Dobson circulation in different QBO phases. Flury et al. (2013) have shown that the upward transport in the lower stratosphere increases during the easterly QBO (30 hPa). Thus, the volcanic aerosols would be less spread vertically in the equatorial stratosphere when transport in the low/mid-stratosphere is weaker during the westerly QBO (Flury et al., 2013). We also note that this volcanic activity pattern does not come from individual big eruptions in the westerly QBO, but eruptions are more or less evenly distributed to both QBO phases (not shown).

We have shown earlier (Maliniemi et al., 2016) that the positive correlation between geomagnetic activity and NAO was mainly observed in the easterly QBO phase. Roy et al. (2016) showed that the combined effect of QBO and geomagnetic activity produced a greatly amplified response at high latitudes. The aa* signal also differs quite dramatically between the two QBO phases. The aa* signal in the easterly QBO is similar to the result in Fig. A3, resembling the (slightly shifted) positive NAO pattern. In the westerly QBO there is a significant signal in the Pacific sector with large negative anomalies over Alaska and the Northeast Pacific and a weaker positive anomaly in the West Pacific. In the Atlantic sector no anomalies are significant for the QBO westerly phase. We propose that the QBO dependence of aa* may also be related to the strength of the Brewer-Dobson circulation. Stronger Brewer-Dobson circulation in the easterly QBO (Flury et al., 2013) transports more ozone to the high latitudes and enhances the downwelling of both ozone and NO_x inside the polar vortex. Thus, during active geomagnetic periods it is expected that more ozone would be destroyed due to the geomagnetic effects in the easterly than in the westerly QBO, making the geomagnetic effect stronger in the easterly QBO phase.

For SSN the signal in the easterly QBO is similar to Fig. A3 but the negative anomaly in Eurasia is now stronger. In the westerly QBO the signal in the Pacific is the same as in the easterly phase and in Fig. A3, but the negative anomalies in Eurasia are smaller and differently located. The similarity of patterns related to SSN in different QBO phases in the Pacific side are interesting and strongly suggests that the stratospheric pathway does not have a significant role in them. Instead, the signal likely has a tropospheric origin due to the bottom-up mechanism described earlier (Meehl et al., 2008). On the other hand, changes in Eurasia and Europe are quite different in different QBO phases, which might suggest a stratospheric pathway similarly as with ENSO.

Fig. A6 shows the QBO phase separation for late winter. As mentioned earlier, the QBO phase is determined from Dec/Jan average. The QBO modulation of ENSO pattern in late winter is rather small. The Atlantic sector is similar in both QBO phases, unlike in early winter (see Fig. A5). The patterns in Fig. A6 are roughly similar but somewhat stronger (weaker) and more (less) significant in the Atlantic (Pacific) side in the westerly QBO and vice versa in the easterly phase. These ENSO patterns in different QBO phases in Figs. A5 and A6 are consistent with earlier observations by Calvo et al. (2009). They showed that warm ENSO events weaken the polar vortex in late winter regardless of the QBO phase. In addition, the easterly QBO advances the onset of the warm ENSO signal, whereas the westerly QBO delays it earlier in winter. This supports our findings when noting the differences in Fig. A5.

Interestingly, volcanic activity is much stronger in the westerly QBO than in the easterly phase, or in early winter in either QBO phase. It greatly resembles the positive NAO pattern supporting the hypothesis of a stronger volcanic effect due to reduced scattering of volcanic aerosols in the equatorial stratosphere with a weaker vertical transport in the westerly QBO as discussed more detail above. The aa* pattern in the easterly QBO reproduces the overall pattern obtained in Fig. A4, while the westerly QBO shows a different pattern with insignificant positive anomaly over the Arctic and negative anomalies around it. Comparing Figs. A5 and A6, it looks as if the aa* pattern of early winter (outside the Pacific) is slightly rotated eastwards in late winter. These patterns related to aa* and volcanic activity in Figs. A5 and A6 support the hypothesis that their forcing comes purely from the stratosphere (in both Dec/Jan and Feb/Mar) and are strongly modulated by the QBO.

The pattern related to SSN in the easterly QBO (see Fig. A6) also resembles the pattern in Fig. A4 and shows a strong positive NAO pattern with a negative anomaly over the Arctic and a positive (but not very significant) anomaly over Europe and the Atlantic. In the westerly QBO there is a more or less opposite overall signal with a positive but

less significant pattern over the Arctic and negative signals in the lower latitudes. These patterns are consistent with earlier findings of e.g., Labitzke and van Loon (1988) and Lu et al. (2009) showing a strong QBO modulation of sunspot signal in the polar region. Unlike the SSN signal in early/mid-winter this late winter signal is strongly modulated by the QBO, suggesting that the forcing has a stratospheric origin. This supports the top-down mechanism (Kodera and Kuroda, 2002) as discussed earlier in Fig. A4.

5. Long-term zonal wind signal in early and late winter

Results related to zonal wind are shown in Figs. A7-A10. Figs. A7 and A8 show early/mid- and late winter ZW signatures, respectively, without the QBO modulation, and Figs. A9 and A10 the corresponding results with the QBO separation. Overall, the results for ZW agree well with the SLP results, showing enhancements of westerlies in regions where pressure gradient is negative northwards.

Zonal wind signal to ENSO in the Pacific sector is very similar in both early and late winter (see Fig. A7 and A8). There are large positive anomalies across the Central Pacific from Japan to California. There is also a less extensive negative ZW anomaly in the West Coast of Canada and Alaska. In the Atlantic sector there is a weak positive anomaly from Caribbean towards North Africa in early/mid-winter which is strengthened in late winter. There is also a strong negative anomaly from Canada to Scandinavia in late winter. These patterns match well with the SLP signals observed in Figs. A3 and A4 where the Atlantic sector shows a strong negative NAO pattern in related to ENSO especially in late winter. They are essentially in line with the notion above that the Atlantic signal is generated later possibly due to the lag involved in the planetary wave forcing through the stratospheric pathway.

Volcanic activity shows signatures in ZW mainly in the Atlantic sector that are fairly similar in early/mid- and late winter. In early/mid-winter westerlies are enhanced from South Greenland to Great Britain and to the Baltic Sea and weakened from Caribbean to Azores. In late winter these patterns are somewhat decreased and directed more northeast. Again they match well with the SLP signals observed for volcanic activity and show ZW signal resembling the positive NAO pattern.

The signal associated with aa* in early/mid-winter shows an enhancement of westerlies from South Greenland to Great Britain and the Baltic Sea and also from North Japan to the Central Pacific. Westerlies are weakened south of Azores. In late winter the Pacific signal vanishes, whereas in the Atlantic sector both the negative and positive anomaly regions move somewhat northwards. The pattern related to SSN in early winter show weakening of westerlies in the Central Pacific (north of Hawaii) related to the positive SLP anomaly in Fig. A3, and a weak enhancement in the low-latitude Pacific. In late winter this Pacific dipole moves northwards. There is also an enhancement of westerlies in the Atlantic, north of Azores. Overall, ZW signals to aa* and SSN are very different, the former being more significant and systematic in the Atlantic, the latter in the Pacific. This emphasizes the Pacific bottom-up forcing related to SSN.

There are only small differences in the ENSO signal between the two QBO phases in early/mid-winter in the Pacific sector (see Fig. A9 and A10). However, in the Atlantic sector there are clear differences between the two QBO phases. ENSO in the QBO easterly phase has a typical negative NAO ZW pattern, with weakening of westerlies at high latitudes and strengthening of westerlies from Caribbean to Azores. ENSO in the QBO westerly phase instead shows stronger westerlies from Canada to South Europe. In late winter the ENSO signal in the Atlantic (and Pacific) is very similar in the two QBO phases, both showing a negative NAO pattern. These patterns are consistent with ENSO patterns obtained in Figs. A5 and A6 for SLP and support the mechanism described earlier (Calvo et al., 2009).

The signal related to the volcanic activity shows a strong positive NAO type pattern in the Atlantic sector in the QBO westerly phase in both early/mid- and late winter, whereas in the QBO easterly phase no significant patterns are observed. In the Pacific one can also observe a significant pattern in the westerly QBO, especially in late winter. Interestingly, this pattern resembles the pattern observed in the ENSO even though the patterns are not significant in the SLP (see Figs. A5 and A6). The volcanic activity signal in the Atlantic in the westerly QBO supports the hypothesis related to the QBO forcing of volcanic aerosol dispersion, as discussed earlier.

The signal associated to aa* in the QBO easterly phase in early/mid- and late winter shows strengthening of the overall patterns in the Atlantic sector depicted in Figs. A7 and A8. Interestingly, in the westerly QBO the Pacific sector signal to aa* is again stronger than in the easterly QBO showing stronger westerlies in the North Pacific in early/mid-winter and west of Hawaii in late winter. The Central Atlantic shows a more negative ZW pattern in late winter but statistical significance is only reached in a small area.

For SSN there is not much difference in early/mid-winter between the two QBO phases in the Pacific sector, both showing weakening of westerlies north of Hawaii. Again, this suggests that the SSN signal in the Pacific sector is not mediated through the stratosphere and is due to the tropospheric bottom-up forcing. However, in late winter the patterns are very different. In the easterly QBO the Atlantic sector resembles a positive NAO pattern, while there is no signal in the Pacific sector. In the westerly QBO the westerlies are weakened all around the Arctic Circle and strengthened in the North Pacific and north of Caribbean. These ZW patterns are consistent with the results obtained with SLP and the top-down mechanism (Kodera and Kuroda, 2002).

6. Conclusions

In this paper we have studied the dependence of winter sea-level pressure and zonal wind on ENSO, volcanic activity, geomagnetic activity and sunspot activity, using the multilinear autoregressive method over the time period 1868–2014. The QBO phase (30 hPa height) modulates the signal of all explaining variables, which suggests that the state of the stratosphere affects the mediation of several signals. In addition, the time of the winter (early/mid-winter: Dec/Jan, late winter: Feb/Mar) has a notable role, which suggests that lagged responses are present in the system. This study uses several different drivers in different conditions, which allows a simultaneous comparison of potential sources of the Northern Hemisphere circulation variability. This is especially true for the two different solar-related forcing parameters, which have not been compared simultaneously in the same regression model before. The key findings are as follows.

1. ENSO produces a hemispheric negative NAM pattern, which is considerably stronger in the Atlantic sector in late winter. The ENSO response in the Atlantic is mediated by planetary wave forcing of the stratosphere/upper troposphere (Huang et al., 1998; Ineson and Scaife, 2009). Our results suggest that there is a lag in the response in the Atlantic sector relative to the direct tropospheric forcing in the North Pacific, which is quite similar in the different QBO phases and in both early/mid- and late winter. QBO modulates the ENSO signal so that it becomes significant in the Atlantic sector already in early/mid-winter. The ENSO effect in the easterly QBO phase resembles a negative NAO pattern. The weaker polar vortex during the easterly QBO (Holton and Tan, 1980; Maliniemi et al., 2016) advances the mediation of a negative NAO signal to the Atlantic sector (Ineson and Scaife, 2009) and is observed earlier than without QBO modulation. In late winter when the Holton-Tan mechanism is no longer significant (Lu et al., 2014; Maliniemi et al., 2016) a negative NAO signal is rather similar in the two QBO phases. This QBO modulation of ENSO teleconnection to the Atlantic sector verifies the modeling study by Calvo et al. (2009), both in early/mid- and late winter.

2. The typical positive NAO pattern related to volcanic activity becomes more clear in the westerly QBO phase, especially in late winter. We suggest that this is due to the weaker Brewer-Dobson circulation in the westerly QBO (Flury et al., 2013), which mixes volcanic aerosols less effectively, leaving them mainly to the lower equatorial stratosphere. This would lead to a stronger infrared absorption by these aerosols in the lower equatorial stratosphere, to larger equator-to-pole temperature gradients and a stronger polar vortex (Robock, 2000; Otterå et al., 2010).
3. The geomagnetic activity (energetic particle precipitation) signature in both early/mid- and late winter is modulated by the QBO phase. Geomagnetic activity produces a significant circulation pattern mainly during the easterly QBO. It represents a dipole pressure pattern similar to the positive NAO pattern, although in late winter it is shifted towards the pole. The geomagnetic activity signal is now verified by a simultaneous consideration of sunspot effects, thus generalizing the earlier studies (Maliniemi et al., 2013, 2016; Roy et al., 2016). A possible explanation to the QBO dependence of the signal to geomagnetic activity is that the Brewer-Dobson circulation is stronger in easterly QBO (Flury et al., 2013). This enhances the transport of ozone to high latitudes (Li and Tung, 2014) and the downwelling of NO_x (produced by particle precipitation (Funke et al., 2014)) inside the polar vortex (Baldwin et al., 2001). This would lead to a larger ozone loss for a given level of geomagnetic activity in the QBO easterly phase compared to the westerly QBO, and as so to stronger polar vortex due to the stratospheric cooling (Baumgaertner et al., 2011).
4. The pattern of the signal due to sunspots (or any other solar driver like TSI or EUV/UV co-varying with sunspots) is very different between early/mid- and late winter. The positive NAO pattern due to SSN in late winter, which is mainly obtained in the easterly QBO phase (in agreement with, e.g., Labitzke and van Loon, 1988; Lu et al., 2009), suggests for the top-down mechanism originating in the stratosphere by enhanced solar UV heating (Kodera and Kuroda, 2002). On the other hand, the positive SLP signature in Aleutian in early winter is only marginally modulated by the QBO, which suggests that the stratospheric variability does not have an effect on it. Rather, it supports the bottom-up mechanism, which is directly forced from the troposphere by enhanced heating in the tropical Pacific (e.g., Meehl et al., 2008). These results related to sunspot activity during early/mid- and late winter in different regions and in different QBO phases verify the different earlier findings (Gray et al., 2010, and multiple references therein) under a common global setting.

Appendix A. acknowledgments

We thank all data providers: The Met Office for SLP data (http://www.metoffice.gov.uk/hadobs/hadslp2), NOAA physical science division for the 20th century reanalysis data (https://www.esrl.noaa.gov/psd/data/gridded/data.20thC_ReanV2.html) and for the nino3.4 (http://www.esrl.noaa.gov/psd/data/correlation/nina34.data), KNMI Climate Explorer (http://climexp.knmi.nl) for the QBO data, NASA for the stratospheric aerosol optical depth data (http://data.giss.nasa.gov/modelforce/strataer), The International Service of Geomagnetic Indices (http://isgi.latmos.ipsl.fr) for the aa index and the Solar Influences Data Analysis Center (http://sidc.oma.be/sunspot-data) for the sunspot data (version 1). All data used in this study are available free of charge. We acknowledge the financial support by the Academy of Finland to the ReSoLVE Center of Excellence (project no. 272157) as well as to projects no. 257403 and 292712.

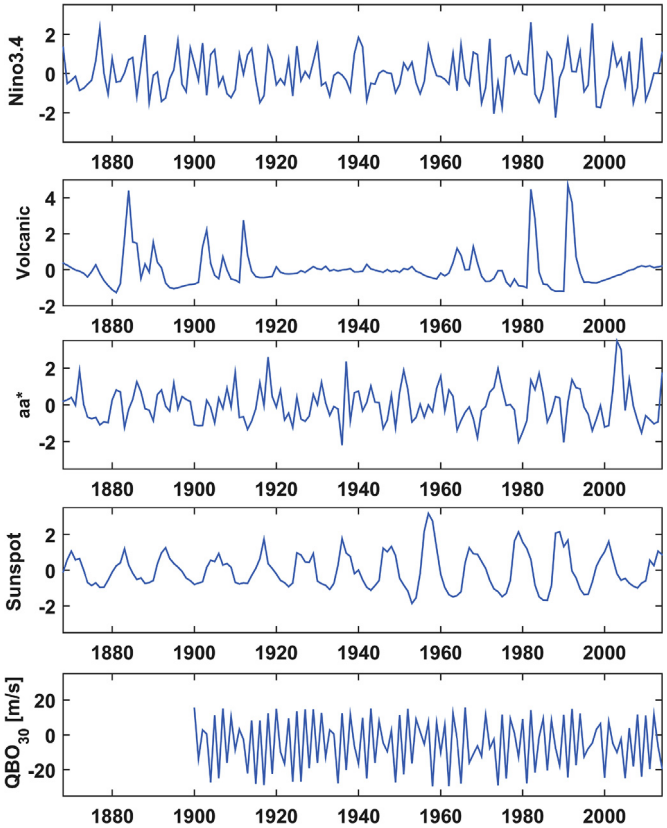

Fig. A1. Dec/Jan average time series of ENSO (top), volcanic activity (second), geomagnetic activity (aa*, third), sunspot number (SSN, fourth) and QBO 30 hPa (bottom). ENSO, volcanic activity, aa* and SSN are detrended with smoothly changing trend (31 year window) and standardized.

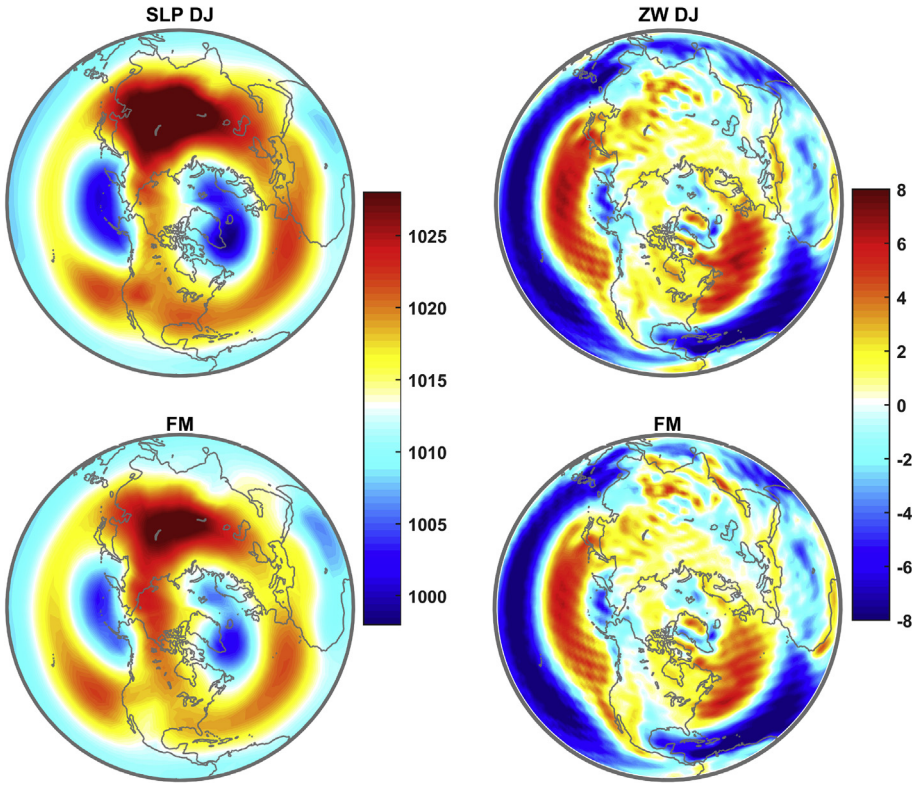

Fig. A2. Top: Dec/Jan climatologies of SLP (left) and surface ZW (right) over the Northern Hemisphere during 1868–2014. Bottom: Feb/Mar climatologies of SLP (left) and ZW (right) over the Northern Hemisphere during 1869–2014.

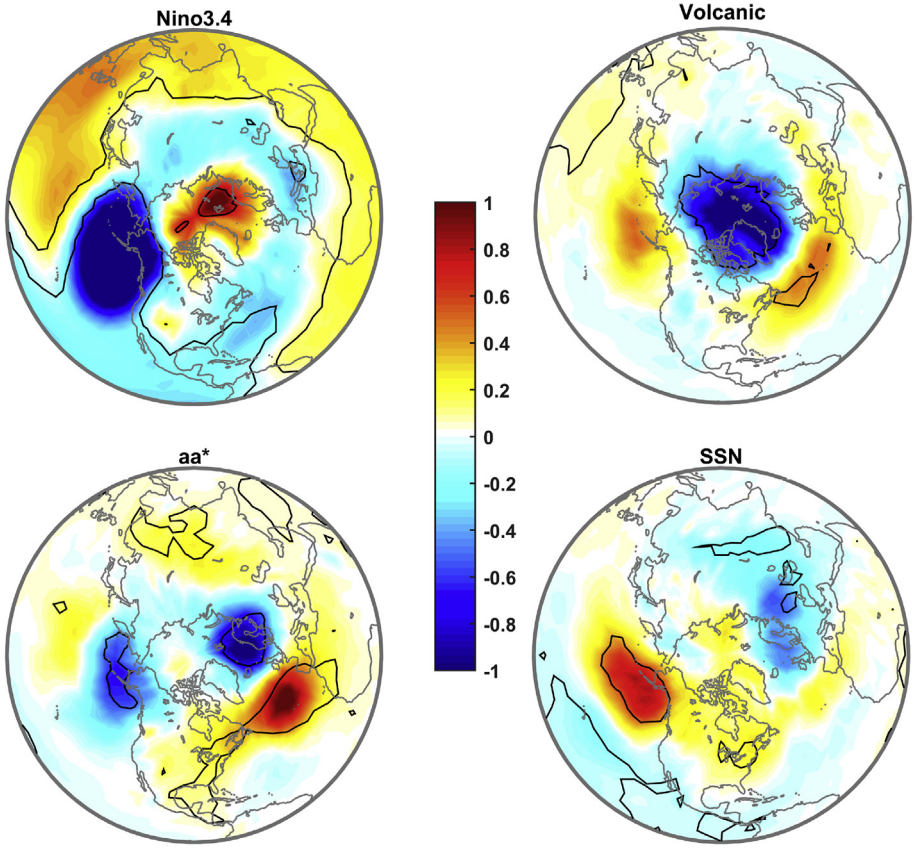

Fig. A3. Regression coefficients of ENSO (top left), volcanic activity (top right), geomagnetic activity (aa*, bottom left) and sunspot number (SSN, bottom right) for SLP in early winter (Dec/Jan) during 1868–2014. Each map shows the variation in SLP (hPa) related to one standard deviation increase in related regression coefficient. Black lines represent the p-value of 0.05.

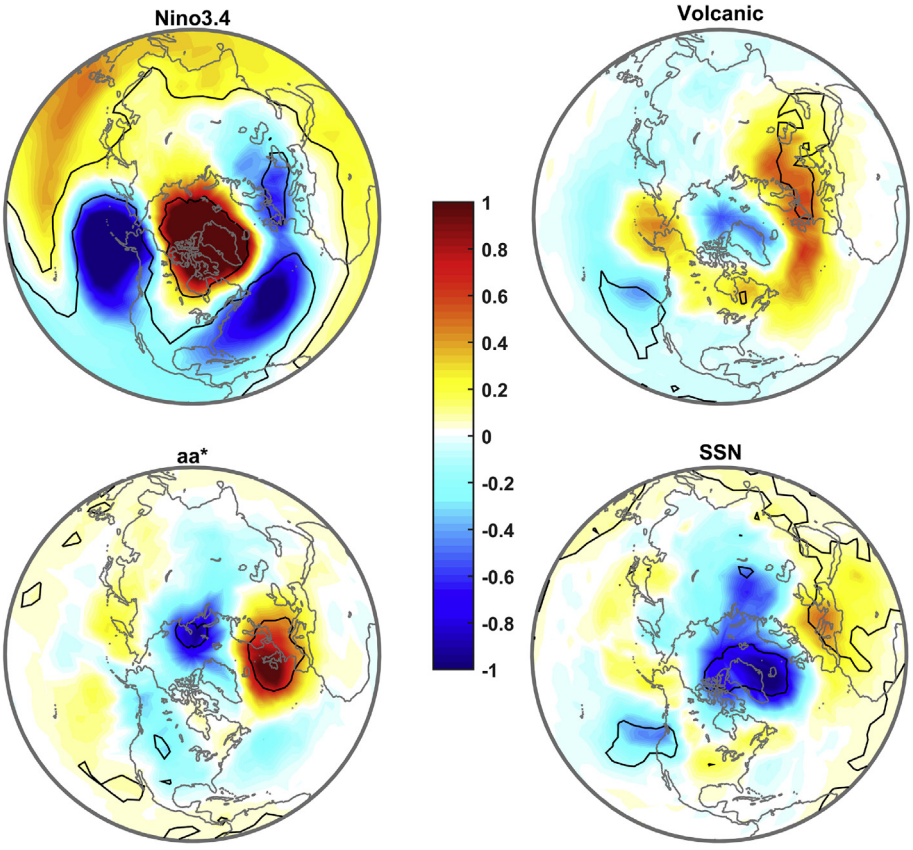

Fig. A4. Same as Fig. A3 but for late winter (Feb/Mar) during 1869–2014.

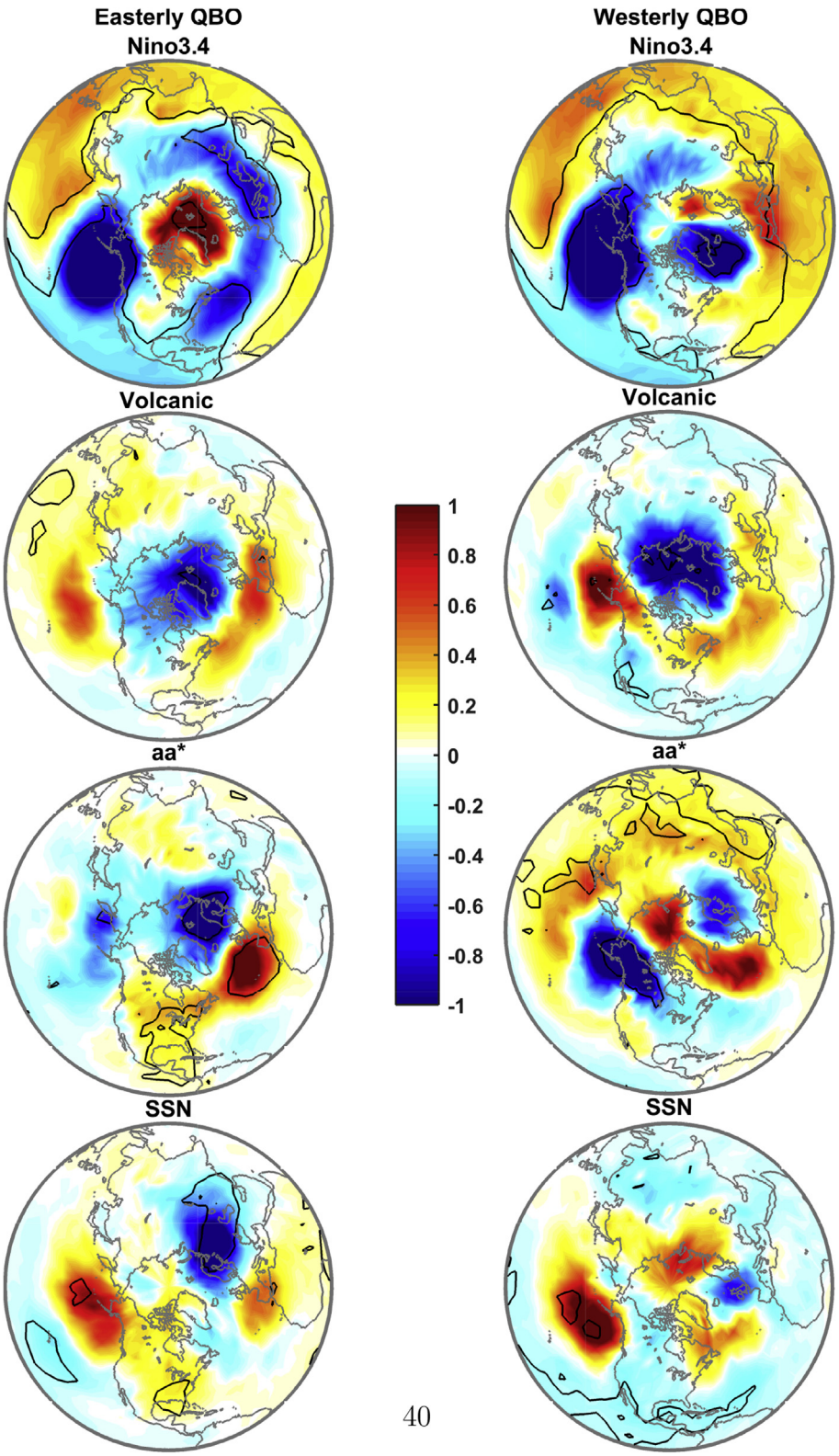

Fig. A5. Same as Fig. A3 for SLP in early winter but data separated to easterly (left) and westerly QBO (right) times during 1900–2014.

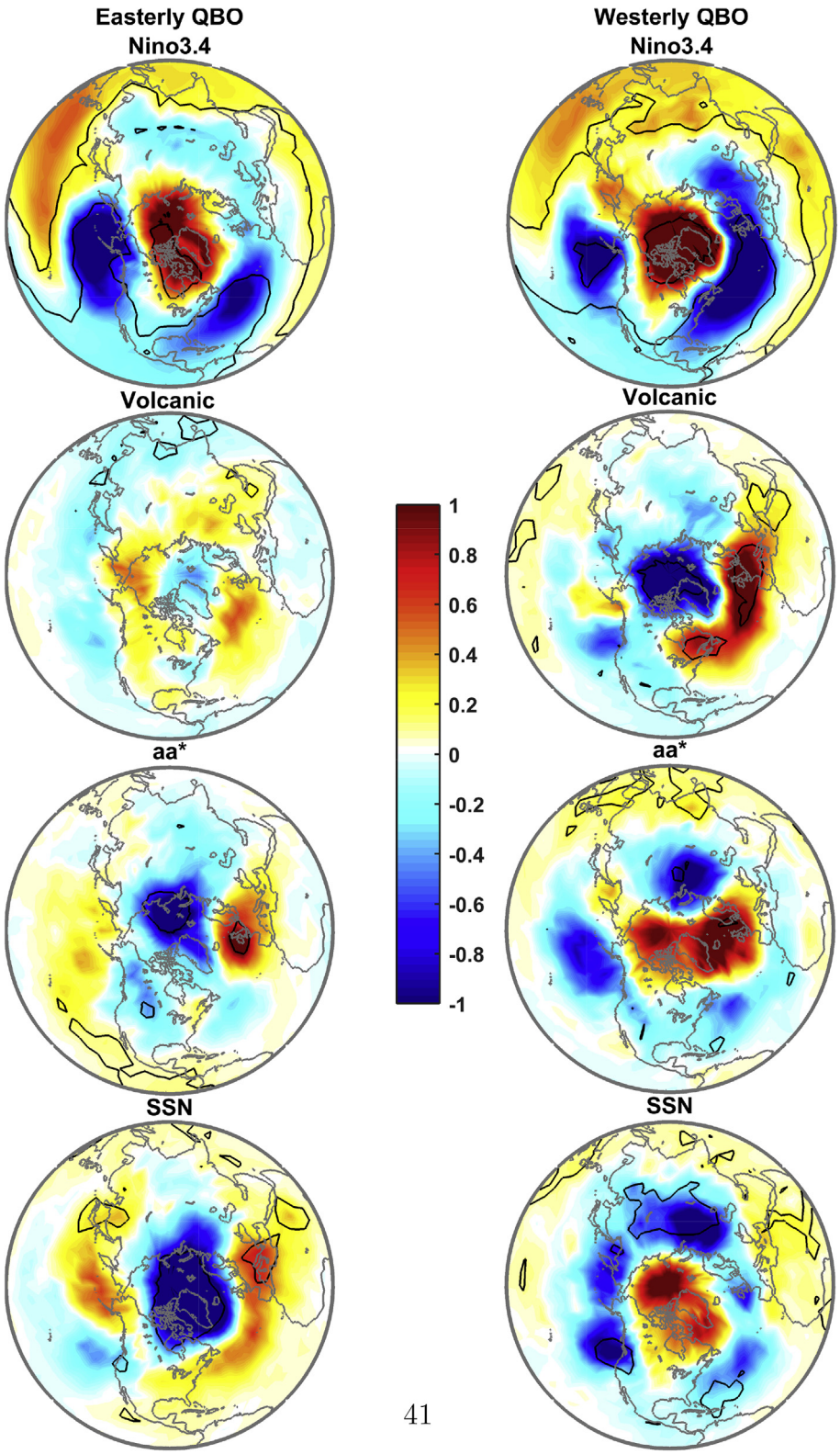

Fig. A6. Same as Fig. A5 but for late winter during 1901–2014.

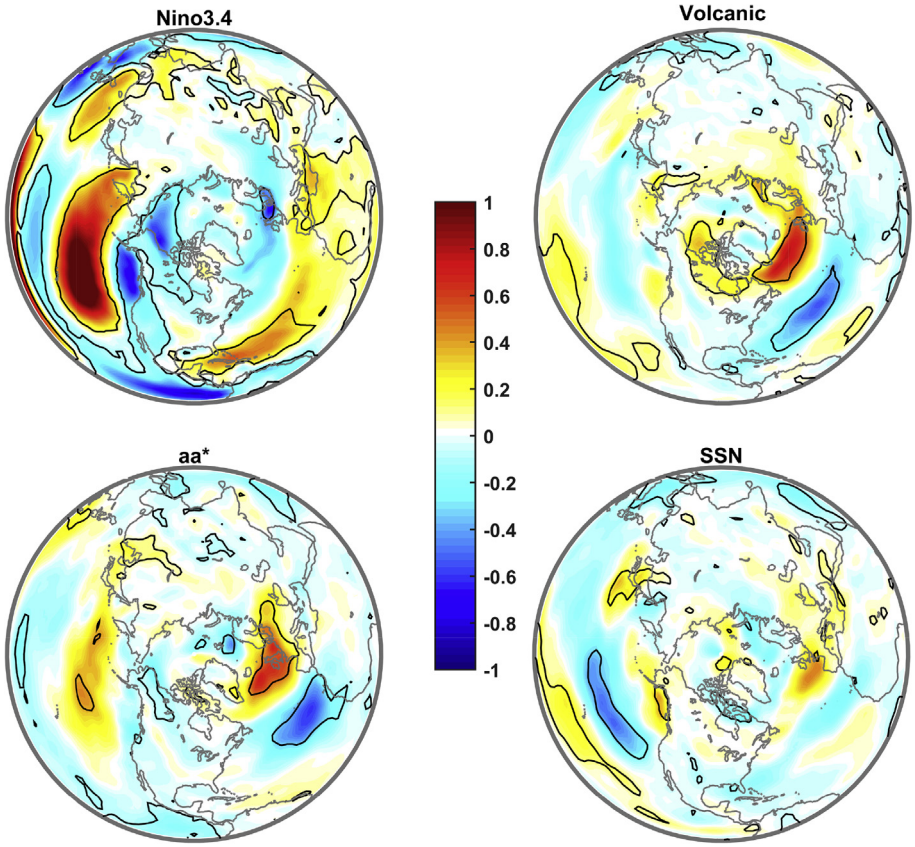

Fig. A7. Regression coefficients of ENSO (top left), volcanic activity (top right), geomagnetic activity (aa*, bottom left) and sunspot number (SSN, bottom right) for surface ZW in early winter (Dec/Jan) during 1868–2014. Each map shows the variation in westerly ZW (m/s) related to one standard deviation increase in related regression coefficient. Black lines represent the p-value of 0.05.

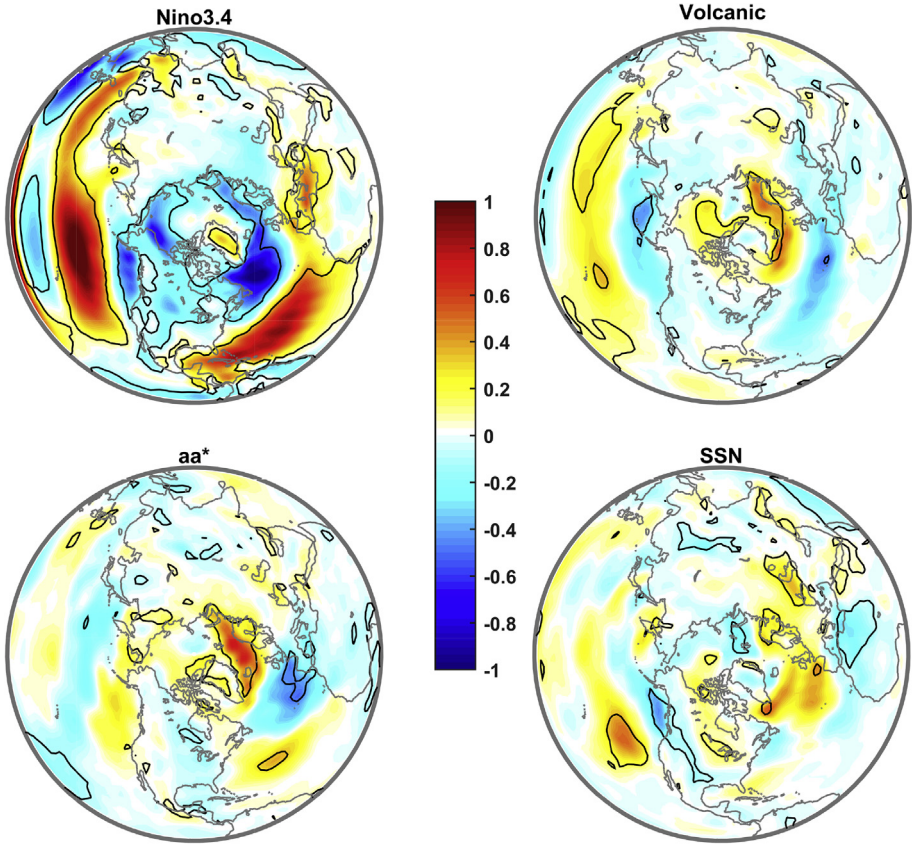

Fig. A8. Same as Fig. A7 but for late winter during 1869–2014.

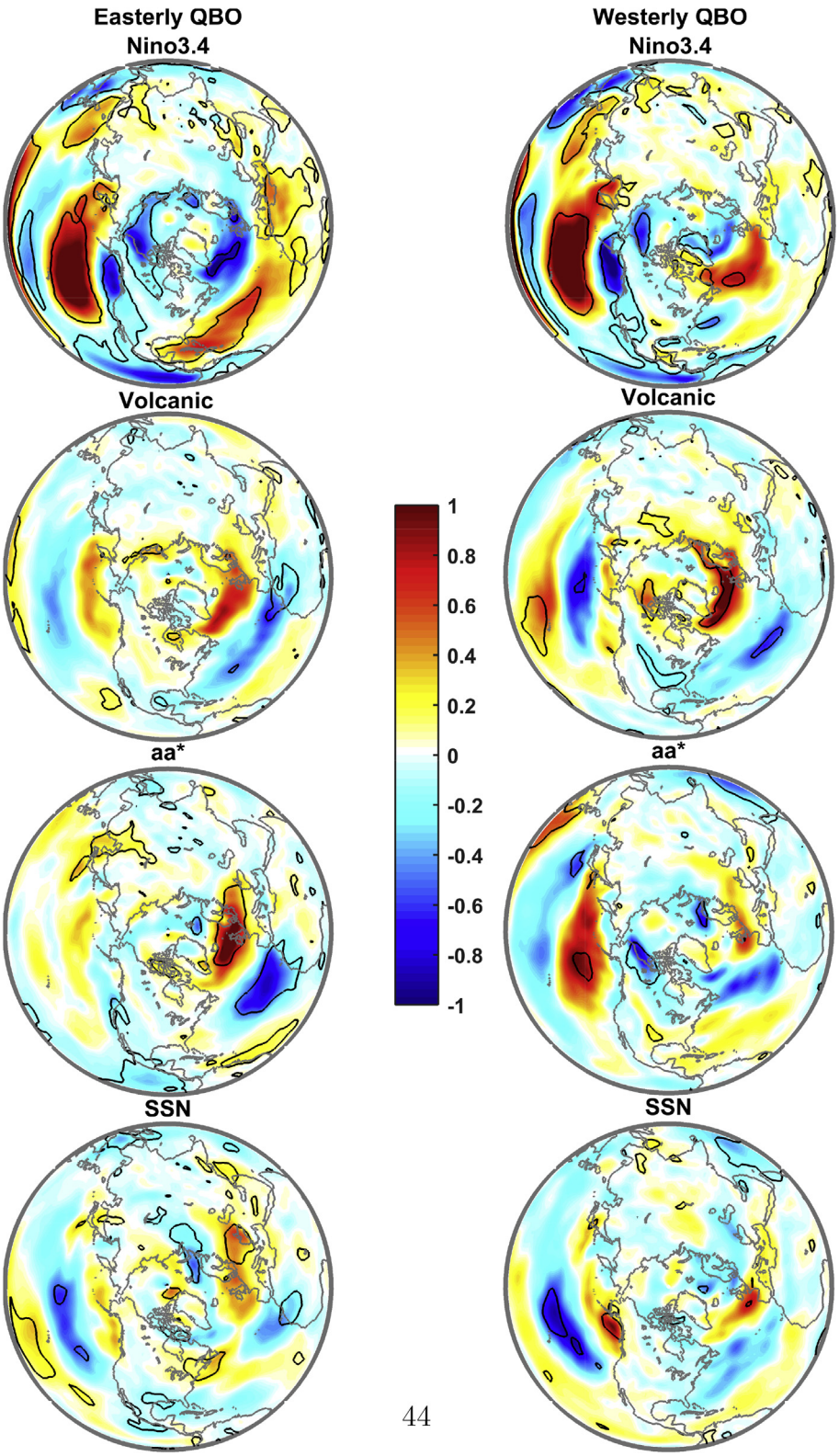

Fig. A9. Same as Fig. A7 for surface ZW in early winter but data separated to easterly (left) and westerly QBO (right) times during 1900–2014.

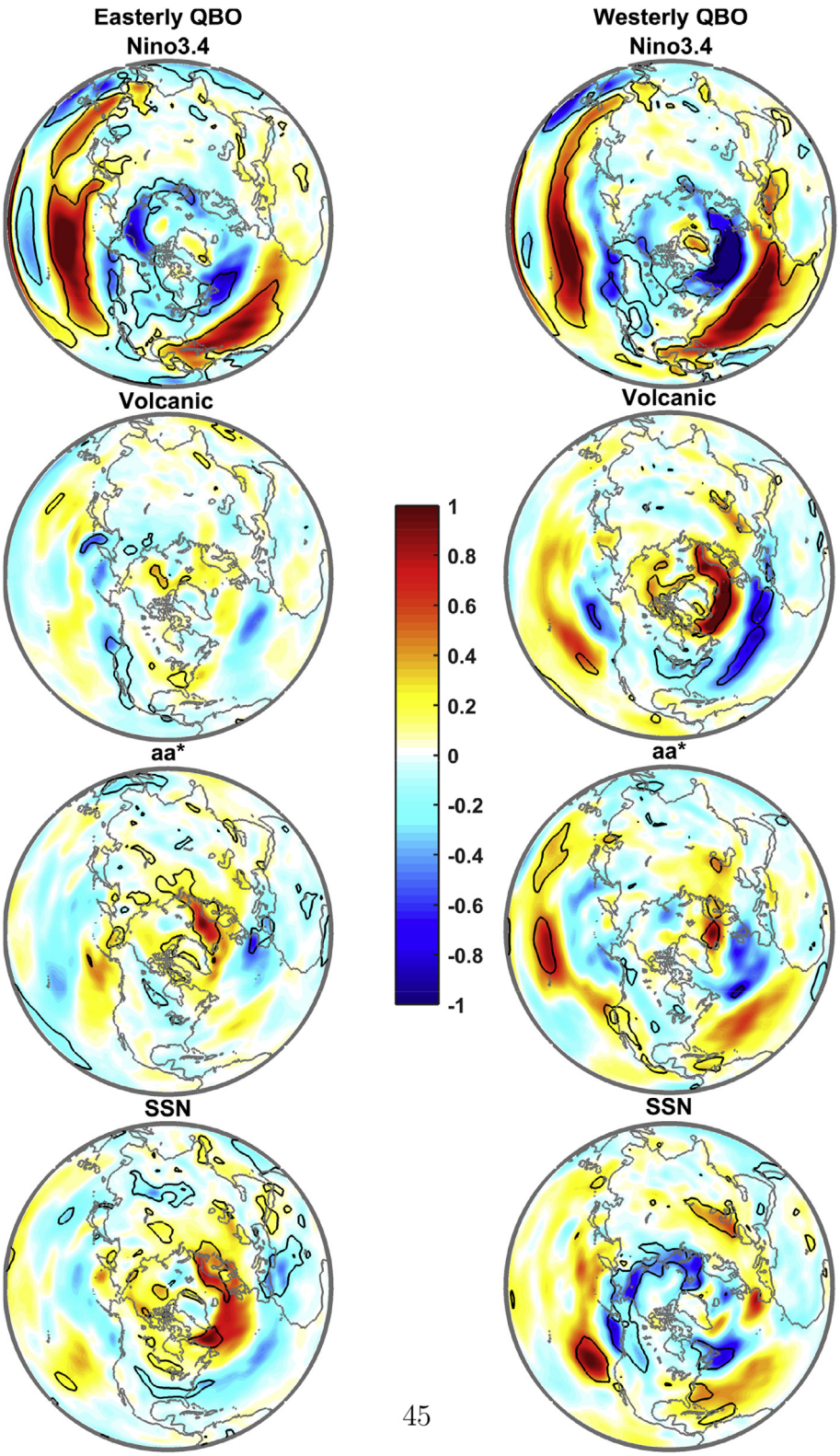

Fig. A10. Same as Fig. A9 but for late winter during 1901–2014.

References

Allan, R., Ansell, T., 2006. A new globally complete monthly historical gridded mean sea level pressure dataset (HadSLP2): 1850 2004. J. Clim. 19, 5816.

Andersson, M.E., Verronen, P.T., Rodger, C.J., Clilverd, M.A., Seppälä, A., Oct. 2014. Missing driver in the Sun-Earth connection from energetic electron precipitation impacts mesospheric ozone. Nat. Commun. 5, 5197.

Anstey, J.A., Shepherd, T.G., 2014. High-latitude influence of the quasi-biennial oscillation. Q. J. R. Meteorol. Soc. 140.

Arsenovic, P., Rozanov, E., Stenke, A., Funke, B., Wissing, J.M., Mursula, K., Tummon, F., Peter, F., Apr. 2016. The influence of middle range energy electrons on atmospheric chemistry and regional climate. J. Atmos. Sol. Terr. Phys. 149, 180–190.

Asikainen, T., Ruopsa, M., Mar. 2016. Solar wind drivers of energetic electron precipitation. J. Geophys. Res. 121, 2209–2225.

Baldwin, M.P., Dunkerton, T.J., Oct. 2001. Stratospheric harbingers of anomalous weather regimes. Science 294, 581–584.

Baldwin, M.P., Gray, L.J., Dunkerton, T.J., Hamilton, K., Haynes, P.H., Randel, W.J., Holton, J.R., Alexander, M.J., Hirota, I., Horinouchi, T., Jones, D.B.A., Kinnersley, J.S., Marquardt, C., Sato, K., Takahashi, M., May 2001. The quasi-biennial oscillation. Rev. Geophys. 39, 179–229.

Baumgaertner, A.J.G., Seppälä, A., Jöckel, P., Clilverd, M.A., May 2011. Geomagnetic activity related NO_x enhancements and polar surface air temperature variability in a chemistry climate model: modulation of the NAM index. Atmos. Chem. Phys. 11, 4521–4531.

Bell, C.J., Gray, L.J., Charlton-Perez, A.J., Joshi, M.M., Scaife, A.A., 2009. Stratospheric communication of el niño teleconnections to european winter. J. Clim. 22, 4083.

Brönnimann, S., Annis, J.L., Vogler, C., Jones, P.D., 2007a. Reconstructing the quasi-biennial oscillation back to the early 1900s. Geophys. Res. Lett. 34, 22805 Nov.

Brönnimann, S., Xoplaki, E., Casty, C., Pauling, A., Luterbacher, J., 2007b. ENSO influence on Europe during the last centuries. Clim. Dynam. 28, 181–197 Feb.

Calvo, N., Giorgetta, M.A., Garcia-Herrera, R., Manzini, E., 2009. Nonlinearity of the combined warm enso and qbo effects on the northern hemisphere polar vortex in maecham5 simulations. J. Geophys. Res. 114 (D13).

Cleveland, W.S., Devlin, S.J., 1988. Locally-weighted regression: an approach to regression analysis by local fitting. J. Am. Stat. Assoc. 83, 596–610.

Cochrane, D., Orcutt, G.H., 1949. Application of least squares regression to relationships containing auto-correlated error terms. J. Am. Stat. Assoc. 44, 32–61.

Compo, G.P., Whitaker, J.S., Sardeshmukh, P.D., Matsui, N., Allan, R.J., Yin, X., Gleason, B.E., Vose, R.S., Rutledge, G., Bessemoulin, P., Brönnimann, S., Brunet, M., Crouthamel, R.I., Grant, A.N., Groisman, P.Y., Jones, P.D., Kruk, M.C., Kruger, A.C., Marshall, G.J., Maugeri, M., Mok, H.Y., Nordli-Ross, T.F., Trigo, R.M., Wang, X.L., Woodruff, S.D., Worley, S.J., 2011. The twentieth century reanalysis project. Q. J. R. Meteorol. Soc. 137 (654).

Cubasch, U., Voss, R., Hegerl, G.C., Waszkewitz, J., Crowley, T.J., Nov 1997. Simulation of the influence of solar radiation variations on the global climate with an ocean-atmosphere general circulation model. Clim. Dynam. 13 (11), 757–767.

Ermolli, I., Matthes, K., Dudok de Wit, T., Krivova, N.A., Tourpali, K., Weber, M., Unruh, Y.C., Gray, L., Langematz, U., Pilewskie, P., Rozanov, E., Schmutz, W., Shapiro, A., Solanki, S.K., Woods, T.N., 2013. Recent variability of the solar spectral irradiance and its impact on climate modelling. Atmos. Chem. Phys. 13, 3945–3977 Apr.

Feynman, J., 1982. Geomagnetic and solar wind cycles, 19001975. J. Geophys. Res. 87, 6153–6162.

Fischer, E.M., Luterbacher, J., Zorita, E., Tett, S.F.B., Casty, C., Wanner, H., Mar. 2007. European climate response to tropical volcanic eruptions over the last half millennium. Geophys. Res. Lett. 34, 5707.

Flury, T., Wu, D.L., Read, W.G., May 2013. Variability in the speed of the Brewer-Dobson circulation as observed by Aura/MLS. Atmos. Chem. Phys. 13, 4563–4575.

Frame, T.H.A., Gray, L.J., Apr. 2010. The 11-yr solar cycle in ERA-40 data: an update to 2008. J. Clim. 23, 2213–2222.

Funke, B., López-Puertas, M., Stiller, G.P., Clarmann, T., Apr. 2014. Mesospheric and stratospheric NO_y produced by energetic particle precipitation during 2002-2012. J. Geophys. Res. 119, 4429–4446.

Fytterer, T., Mlynczak, M.G., Nieder, H., Pérot, K., Sinnhuber, M., Stiller, G., Urban, J., 2015a. Energetic particle induced intra-seasonal variability of ozone inside the antarctic polar vortex observed in satellite data. Atmos. Chem. Phys. 15, 3327–3338.

Fytterer, T., Santee, M.L., Sinnhuber, M., Wang, S., 2015b. The 27day solar rotational effect on mesospheric nighttime oh and o3 observations induced by geomagnetic activity. J. Geophys. Res. 120, 7926–7936.

Gray, L.J., Beer, J., Geller, M., Haigh, J.D., Lockwood, M., Matthes, K., Cubasch, U., Fleitmann, D., Harrison, G., Hood, L., Luterbacher, J., Meehl, G.A., Shindell, D., van Geel, B., White, W., Oct. 2010. Solar influences on climate. Rev. Geophys. 48 RG4001.

Gray, L.J., Scaife, A.A., Mitchell, D.M., Osprey, S., Ineson, S., Hardiman, S., Butchart, N., Knight, J., Sutton, R., Kodera, K., Dec. 2013. A lagged response to the 11 year solar cycle in observed winter Atlantic/European weather patterns. J. Geophys. Res. 118, 13405–13420.

Gray, L.J., Woollings, T.J., Andrews, M., Knight, J., Mar. 2016. 11-year solar cycle signal in the NAO and Atlantic/European blocking. Q. J. Roy. Meteorol. Soc. 142, 1890–1903.

Haigh, J.D., Oct. 2007. The Sun and the Earth's climate. Living Rev. Sol. Phys. 4, 2.

Hansen, F., Matthes, K., Wahl, S., Feb. 2016. Tropospheric qbo-enso interactions and differences between the atlantic and pacific. J. Clim. 29, 1353–1368.

Herceg-Buli, I., Mezzina, B., Kucharski, F., Ruggieri, P., King, M.P., 2017. Wintertime enso influence on late spring european climate: the stratospheric response and the role of north atlantic sst. Int. J. Climatol. 37, 87–108.

Holton, J.R., 2004. An Introduction to Dynamic Meteorology. Cambridge University Press, UK.

Holton, J.R., Tan, H.-C., Oct. 1980. The influence of the equatorial quasi-biennial oscillation on the global circulation at 50 mb. J. Atmos. Sci. 37, 2200–2208.

Holton, J.R., Tan, H.-C., 1982. The quasi-biennial oscillation in the Northern Hemisphere lower stratosphere. J. Meteorol. Soc. Jpn. 60, 140–148.

Huang, J., Higuchi, K., Shabbar, A., 1998. The relationship between the north atlantic oscillation and el niÃ ± o-southern oscillation. Geophys. Res. Lett. 25 (14), 2707–2710.

Ineson, S., Scaife, A.A., Jan. 2009. The role of the stratosphere in the European climate response to El Niño. Nat. Geosci. 2, 32–36.

Ineson, S., Scaife, A.A., Knight, J.R., Manners, J.C., Dunstone, N.J., Gray, L.J., Haigh, J.D., Nov. 2011. Solar forcing of winter climate variability in the Northern Hemisphere. Nat. Geosci. 4, 753–757.

Kidston, J., Scaife, A.A., Hardiman, S.C., Mitchell, D.M., Butchart, N., Baldwin, M.P., Gray, L.J., Jun. 2015. Stratospheric influence on tropospheric jet streams, storm tracks and surface weather. Nat. Geosci. 8, 433–440.

Kodera, K., Kuroda, Y., Dec. 2002. Dynamical response to the solar cycle. J. Geophys. Res. 107, 4749.

Labitzke, K., van Loon, H., Mar. 1988. Associations between the 11-year solar cycle, the QBO and the atmosphere. I - the troposphere and stratosphere in the Northern Hemisphere in winter. J. Atmos. Sol. Terr. Phys. 50, 197–206.

Li, K.-F., Tung, K., 2014. Quasibiennial oscillation and solar cycle influences on winter arctic total ozone. J. Geophys. Res. Atmos. 119 (10), 5823–5835.

Lockwood, M., Fröhlich, C., 2007. Recent oppositely directed trends in solar climate forcings and the global mean surface air temperature. Proc. R. Soc. A 463 (2086), 2447–2460.

Lu, H., Bracegirdle, T.J., Phillips, T., Bushell, A., Gray, L., Mar. 2014. Mechanisms for the Holton-Tan relationship and its decadal variation. J. Geophys. Res. 119, 2811–2830.

Lu, H., Gray, L.J., Baldwin, M.P., Jarvis, M.J., Apr. 2009. Life cycle of the QBO-modulated 11-year solar cycle signals in the Northern Hemispheric winter. Q. J. Roy. Meteorol. Soc. 135, 1030–1043.

Lu, H., Jarvis, M.J., Hibbins, R.E., 2008. Possible solar wind effect on the northern annular mode and northern hemispheric circulation during winter and spring. J. Geophys. Res. 113 (D23).

Maliniemi, V., Asikainen, T., Mursula, K., 2014. Spatial distribution of Northern Hemisphere winter temperatures during different phases of the solar cycle. J. Geophys. Res. 119.

Maliniemi, V., Asikainen, T., Mursula, K., 2016. Effect of geomagnetic activity on the northern annular mode: qbo dependence and the holton-tan relationship. J. Geophys. Res. 121.

Maliniemi, V., Asikainen, T., Mursula, K., Seppälä, A., 2013. QBO-dependent relation between electron precipitation and wintertime surface temperature. J. Geophys. Res. 118.

Meehl, G.A., Arblaster, J.M., Branstator, G., van Loon, H., 2008. A coupled air sea response mechanism to solar forcing in the pacific region. J. Clim. 21, 2883.

Mitchell, D.M., Misios, S., Gray, L.J., Tourpali, K., Matthes, K., Hood, L., Schmidt, H., Chiodo, G., ThiÃ©blemont, R., Rozanov, E., Shindell, D., Krivolutsky, A., 2015. Solar signals in cmip-5 simulations: the stratospheric pathway. Q. J. Roy. Meteorol. Soc. 141.

Mursula, K., Lukianova, R., Holappa, L., Mar. 2015. Occurrence of high-speed solar wind streams over the grand modern maximum. Astrophys. J. 801, 30.

Otterå, O.H., Bentsen, M., Drange, H., Suo, L., Oct. 2010. External forcing as a metronome for Atlantic multidecadal variability. Nat. Geosci. 3, 688–694.

Pozo-Vázquez, D., Esteban-Parra, M.J., Rodrigo, F.S., Castro-Díez, Y., Aug. 2001. The association between ENSO and winter atmospheric circulation and temperature in the North atlantic region. J. Clim. 14, 3408–3420.

Robock, A., May 2000. Volcanic eruptions and climate. Rev. Geophys. 38, 191–219.

Roy, I., Asikainen, T., Maliniemi, V., Mursula, K., 2016. Comparing the influence of sunspot activity and geomagnetic activity on winter surface climate. J. Atmos. Sol. Terr. Phys. 149, 167–179.

Roy, I., Haigh, J.D., Nov. 2011. The influence of solar variability and the quasi-biennial oscillation on lower atmospheric temperatures and sea level pressure. Atmos. Chem. Phys. 11, 11679–11687.

Roy, I., Haigh, J.D., Apr. 2012. Solar cycle signals in the Pacific and the issue of timings. J. Atmos. Sci. 69, 1446–1451.

Rozanov, E., Calisto, M., Egorova, T., Peter, T., Schmutz, W., 2012. Influence of the precipitating energetic particles on atmospheric chemistry and climate. Surv. Geophys. 33 (3), 483–501.

Ruzmaikin, A., Feynman, J., 2001. Strength and phase of the solar dynamo during the last

12 cycles. J. Geophys. Res. 106, 15783–15789.
Salby, M.L., Callaghan, P.F., Dec. 2003. Interannual changes of the stratospheric circulation: relationship to ozone and tropospheric structure. J. Clim. 15, 3673–3685.
Sato, M., Hansen, J.E., McCormick, M.P., Pollack, J.B., Dec. 1993. Stratospheric aerosol optical depths, 1850-1990. J. Geophys. Res. 98, 22987–22994.
Seppälä, A., Lu, H., Clilverd, M.A., Rodger, C.J., Mar. 2013. Geomagnetic activity signatures in wintertime stratosphere wind, temperature, and wave response. J. Geophys. Res. 118, 2169–2183.
Seppälä, A., Matthes, K., Randall, C.E., Mironova, I.A., Dec. 2014. What is the solar influence on climate? Overview of activities during CAWSES-II. Prog Earth Planet Sci. 1, 24.
Shindell, D.T., Schmidt, G.A., Mann, M.E., Faluvegi, G., Mar. 2004. Dynamic winter climate response to large tropical volcanic eruptions since 1600. J. Geophys. Res. 109, 5104.
Thiéblemont, R., Matthes, K., Omrani, N.-E., Kodera, K., Hansen, F., Sep. 2015. Solar forcing synchronizes decadal North Atlantic climate variability. Nat. Commun. 6.
Toniazzo, T., Scaife, A.A., Dec. 2006. The influence of ENSO on winter North Atlantic climate. Geophys. Res. Lett. 33, 24704.
van Loon, H., Meehl, G.A., Shea, D.J., Jan. 2007. Coupled air-sea response to solar forcing in the Pacific region during northern winter. J. Geophys. Res. 112, 2108.
Wang, Y.-H., Magnusdottir, G., Stern, H., Tian, X., Yu, Y., Nov. 2012. Decadal variability of the NAO: introducing an augmented NAO index. Geophys. Res. Lett. 39, 21702.